

# Discovery of a Low Mass Bipolar Molecular Outflow from L1014-IRS with the Submillimeter Array

Tyler L. Bourke<sup>1</sup>, Antonio Crapsi<sup>1,2</sup>, Philip C. Myers<sup>1</sup>, Neal J. Evans II<sup>3</sup>, David J. Wilner<sup>1</sup>, Tracy L. Huard<sup>1</sup>, Jes K. Jørgensen<sup>1</sup>, Chadwick H. Young<sup>3</sup>

## ABSTRACT

Using the Submillimeter Array we report the discovery of a compact low mass bipolar molecular outflow from L1014-IRS and confirm its association with the L1014 dense core at 200 pc. Consequently, L1014-IRS is the lowest luminosity ( $L \sim 0.09 L_{\odot}$ ) and perhaps the lowest mass source known to be driving a bipolar molecular outflow, which is one of the smallest known in size ( $\sim 500$  AU), mass ( $< 10^{-4} M_{\odot}$ ), and energetics (e.g., force  $< 10^{-7} M_{\odot} \text{ km s}^{-1} \text{ yr}^{-1}$ ).

*Subject headings:* ISM: individual (L1014, L1014-IRS) – ISM: jets and outflows – stars: formation – stars: low-mass, brown-dwarfs – techniques: interferometric

## 1. Introduction

*Spitzer Space Telescope* observations of the Bok globule L1014, previously classified as starless (Parker 1988), discovered an infrared point source with protostellar colors, L1014-IRS, located near to the globule's dust emission peak (Young et al. 2004). The infrared colors of L1014-IRS are consistent with (i) a protostar or proto-brown-dwarf in L1014 at  $\sim 200$  pc (Leung, Kutner & Mead 1982), as assumed by Young et al. (2004), or (ii) an intermediate mass T Tauri star ( $L \sim 16 L_{\odot}$ ) associated with a background cloud in the Perseus arm at 2.6 kpc.

Assuming that the distance to L1014-IRS is 200 pc, its star plus disk luminosity, assuming isotropic emission, is  $\sim 0.09 L_{\odot}$ , and the best fit to its SED is with a protostar luminosity of  $0.025$

---

<sup>1</sup>Harvard-Smithsonian Center for Astrophysics, 60 Garden Street, Cambridge, MA 02138; tbourke@cfa.harvard.edu

<sup>2</sup>Università degli Studi di Firenze, Dipartimento di Astronomia e Scienza dello Spazio, Largo E. Fermi 5, I-50125 Firenze, Italy

<sup>3</sup>University of Texas at Austin, 1 University Station C1400, Austin, TX 78712-0259

$L_{\odot}$ . If L1014-IRS has the age of a typical Class I protostar of  $\sim 10^5$  yr then it has a substellar mass of only 20-45  $M_{\text{Jup}}$  (Huard et al. 2005). However, no spectroscopic observations exist to determine its mass and accretion rate, and so it is unclear whether L1014-IRS is a young protostar still acquiring a significant fraction of its final mass, or whether it is destined to remain substellar.

More recent observations strongly support the conclusion that L1014-IRS is embedded within L1014 (Crapsi et al. 2005; Huard et al. 2005), however the evidence is still circumstantial. It has not been shown that L1014-IRS has the same local velocity as L1014, nor has an outflow been detected, despite recent searches using CO with single dish telescopes (Visser et al. 2001; Crapsi et al. 2005). In this paper we present Submillimeter Array (SMA) observations of CO  $J = 2 \rightarrow 1$  toward L1014-IRS, to search for a compact outflow and to resolve the distance ambiguity.

## 2. Observations

Observations of L1014 near 230 GHz were obtained with the SMA<sup>1</sup> (Ho et al. 2004) on 2004 August 15 and September 5. Zenith opacities at 225 GHz were typically in the range 0.1-0.2. The observations utilized both 2 GHz wide receiver sidebands, separated by 10 GHz. The SMA correlator was configured with high spectral resolution bands of 512 channels over 104 MHz for the  $^{12}\text{CO}$ ,  $^{13}\text{CO}$  and  $\text{C}^{18}\text{O}$   $J = 2 \rightarrow 1$  lines, providing a channel spacing of  $0.26 \text{ km s}^{-1}$ , with a lower resolution of 3.25 MHz/channel over the remainder of each sideband. Observations of L1014 were interleaved with the quasars BL Lac and J2013+370 for gain calibration. The data were edited and calibrated using the MIR software package adapted for the SMA. Saturn and Uranus were used for passband and flux calibration, respectively. The flux of BL Lac measured on the two days agrees to within 20%, which we take to be the uncertainty in the absolute flux scale. Mapping was performed with the MIRIAD package, resulting in an angular resolution of  $1''.2 \times 1''.0$  (natural weighting). The rms sensitivity was  $\sim 2 \text{ mJy}$  for the continuum, using both sidebands (avoiding the band containing the CO line), and  $\sim 0.1 \text{ Jy beam}^{-1}$  per channel for the line data. The primary FWHM beam of the SMA is  $\sim 55''$  at these frequencies.

## 3. L1014-IRS: A Protostar at 2.6 kpc?

The systemic velocity of L1014 is  $4.2 \text{ km s}^{-1}$  (Crapsi et al. 2005). Behind L1014 lies another cloud with a velocity near  $-40 \text{ km s}^{-1}$  associated with the Perseus arm at 2.6 kpc (Young

---

<sup>1</sup>The Submillimeter Array is a joint project between the Smithsonian Astrophysical Observatory and the Academia Sinica Institute of Astronomy and Astrophysics and is funded by the Smithsonian Institution and the Academia Sinica.

et al. 2004; Crapsi et al. 2005). Emission from the  $J = 1 \rightarrow 0$  lines of  $\text{C}^{18}\text{O}$  and  $\text{N}_2\text{H}^+$ , and the  $J = 2 \rightarrow 1$  line of CS, tracing gas density  $10^{3-5} \text{ cm}^{-3}$ , was not detected at these velocities in a  $\sim 50''$  beam by Crapsi et al. (2005). No CO emission is detected in the SMA data over the velocity range  $[-35, -45] \text{ km s}^{-1}$ , implying that no compact CO emission nor outflow is associated with this velocity component to the level of our sensitivity.

A tentative detection of continuum emission of  $7 \pm 3 \text{ mJy}$  was obtained at the position of L1014-IRS (offset by  $4''.8, 0''.1$  from the phase center) with observations made in the compact configuration, but was not confirmed by the extended array observations. By combining the two data sets and only selecting baseline lengths  $< 50 \text{ k}\lambda$  a similar tentative detection ( $5 \pm 2 \text{ mJy}$ ) is obtained. Young et al. (2004) predict a flux of  $\sim 1\text{--}2 \text{ mJy}$  at  $230 \text{ GHz}$  for the central object (star+disk) of L1014, which is consistent with our results. Recent BIMA imaging at  $\sim 95 \text{ GHz}$  with a  $15\text{--}20''$  synthesised beam shows weak slightly extended emission (Lai et al. in preparation), but no compact component. Young et al. (2004) predict that the emission from a background protostar ( $L \sim 16L_\odot$ ) would be  $\sim 0.6 \text{ Jy}$ , which is clearly ruled out by the SMA observations, and together with the lack of line emission at  $-40 \text{ km s}^{-1}$  (§3), rules out the possibility that L1014-IRS is a distant young star.

#### 4. CO Outflow Associated with L1014-IRS

CO  $J = 2 \rightarrow 1$  (hereafter referred to as CO) emission was detected at velocities blue-shifted and red-shifted with respect to the systemic velocity of L1014 of  $4.2 \text{ km s}^{-1}$ . No emission was detected at the systemic velocity. Figure 1 presents an overview of the CO emission integrated over the blue- and red-shifted velocities, and Fig. 2 presents a position-velocity (P-V) diagram along the main axis of the compact outflow (indicated on Fig. 1(b)). The CO emission is clearly offset from the position of L1014-IRS, in a pattern typical of bipolar molecular outflows, with the blue-shifted emission aligned with the near-infrared scattered light nebula (Huard et al. 2005). Two representations of the data are shown. In Fig. 1(a) the data have been tapered with a  $3''$  Gaussian in order to improve the sensitivity to the fainter emission seen  $\sim 20''$  north and south of the main outflow. The red-shifted emission to the south is clearly visible even at the highest angular resolution. These faint extended emission features are approximately equidistant from the position of L1014-IRS and may be associated with the outflow, perhaps indicating episodic emission. Fig. 1(b) and Fig. 2 show that the inner bipolar emission is very compact: the peaks have projected separation of  $\sim 200 \text{ AU}$  centered on L1014-IRS, the lowest contours are separated by at most  $\sim 700 \text{ AU}$ , and the size of each lobe is only  $\sim 540 \text{ AU}$  ( $0.0026 \text{ pc}$ ) in length.

No emission is detected at the cloud systemic velocity, and the peak emission in both the blue and red lobes are offset by similar amounts from the systemic velocity (Fig. 2). The red-shifted

emission is clearly brighter than the blue-shifted emission by about a factor of two. The brightness asymmetry might arise because L1014-IRS is offset from the density peak, with the red-shifted outflow propagating into denser material resulting in a larger swept up mass, compared to the blue-shifted emission. The core’s column density peak lies  $\sim 10''$  to the south (red-shifted side) of L1014-IRS (Huard et al. 2005), supporting this conjecture. Alternatively, the difference could be due to radiative transfer effects implying a moderate CO opacity (Bally & Lada 1983).

#### 4.1. Molecular Outflow Mass, Kinematics and Dynamics

In order to derive the outflow properties we only consider the compact outflow shown in Fig. 1(b). The nature of the “extended outflow” component is unclear, and requires confirmation, perhaps by combining the SMA data with single-dish data to recover extended missing flux. Observations with the IRAM 30-m telescope of the L1014 cloud in CO  $J = 2 \rightarrow 1$  have recently been made by us. A full analysis of these data are beyond the scope of this paper. However, we can investigate qualitatively the missing flux question. Figure 3 presents a comparison of the SMA and 30-m data. The SMA data have been convolved with a  $4''$  beam (i.e., the approximate area of the outflow), and scaled by the ratio of the beam areas, to approximate the outflow emission detectable by the 30-m in equivalent brightness temperature units. Figures 3(a) and (b) show that no emission and so no missing flux is present at velocities greater than that detected by the SMA. Figure 3(c) indicates that no outflow emission is seen at positions more than  $\sim 11''$  from L1014-IRS in the 30-m data and so no bright large scale outflow is present. In fact, there appears to be residual emission (cloud plus outflow) detected with the 30-m at the position of L1014-IRS some of which could be associated with the SMA outflow. This simple analysis suggests that any missing flux is limited in velocity and extent, and is less than a factor of 3 (Fig. 3(c)).

The outflow properties are calculated in the standard manner (e.g., Cabrit & Bertout 1990). We assume a value for the excitation temperature of 20 K, but values in the range 10–50 K modify the outflow calculations only slightly, less than a factor of two. Two methods are typically used to calculate upper and lower limits to the outflow mass. For the lower limit the emission is assumed to be optically thin, the mass is calculated at each velocity channel and position where outflow emission is observed, and then summed. In the case of the SMA observations we are also missing some emission that has been filtered by the interferometer sampling, and so these values are strict lower limits. However, Fig. 3 suggests that the SMA observations do not suffer greatly from this problem. For the upper limits, a correction for line opacity is required, but we cannot estimate the opacity from our observations as we do not detect  $^{13}\text{CO } J = 2 \rightarrow 1$ , and the sensitivity of the line observations is insufficient to place any meaningful limits on the ratio of  $^{13}\text{CO}$  to  $^{12}\text{CO}$  emission. Thus, we derive only a lower limit to the outflow mass of  $M_{flow} \sim 1.4 \times 10^{-5} M_{\odot}$ , but note that,

if we correct for optical depth using typical values of 2-5 (Levreault 1988), then the upper limits to outflow mass and related properties will be correspondingly greater than our lower limits by similar factors. The mass estimate is consistent with the upper limit of  $2 \times 10^{-3} M_{\odot}$  estimated by Crapsi et al. (2005) from their single-dish data.

For properties relying on a knowledge of the outflow velocity (Momentum  $P$ , Energy  $E$ , Mechanical Luminosity  $L_m$ , and Force  $F_{obs}$ ), lower limits are determined by multiplying the mass in each velocity channel by the relative flow velocity (to the appropriate power) of that channel  $v_{flow} = |V_{flow} - V_{lsr}|$  where  $V_{flow}$  is the observed flow velocity and  $V_{lsr}$  is the systemic velocity. Upper limits are found by assuming that the outflowing gas is moving at the maximum observed velocity  $V_m$ , rather than the relative flow velocity of the channel, corrected for the outflow inclination. From modeling of the infrared scattered light nebula Huard et al. (2005) determine a semi-opening angle of  $\theta \geq 50^\circ$ , and an inclination angle  $i > 60^\circ$ . The correction factor  $1/\cos(i-\theta)$  for inclination effects is then negligible (for  $i \leq 80^\circ$ ). The overlap between the blue and red lobes seen in Fig. 1(b) suggests that  $i$  is closer to  $60^\circ$  than  $> 75^\circ$  (Cabrit & Bertout (1990)). Regardless of the true value for  $i$ , if  $20^\circ < i < 80^\circ$  then the correction for inclination is negligible due to the large observed opening angle. Therefore, for the upper limit values we use the observed maximum flow velocity of  $3.6 \text{ km s}^{-1}$  for  $V_m$ , assuming no correction is needed for inclination. In this way we find  $P = 2.4 - 5.0 \times 10^{-5} M_{\odot} \text{ km s}^{-1}$ ;  $E = 0.24 - 1.6 \times 10^{-4} M_{\odot} \text{ km}^2 \text{ s}^{-2}$ ;  $L_m = 0.34 - 2.8 \times 10^{-5} L_{\odot}$ ; and  $F_{obs} = 3.4 - 7.1 \times 10^{-8} M_{\odot} \text{ km s}^{-1} \text{ yr}^{-1}$ . If correction factors for opacity of  $\sim 3$  and missing flux of  $\sim 3$  (Fig. 3) are assumed, then the maximum values for  $P, E, L_m$  and  $F_{obs}$  will increase by about an order of magnitude.

The outflow mass loss rate  $\dot{M}_{out}$  can be estimated directly from the mass and age  $t_{flow}$ . Typically  $t_{flow} \sim t_d$  (the dynamical time) is assumed, which may not be reasonable (Parker et al. 1991);  $t_d$  is a lower limit to the outflow age. Assuming  $t_{flow} \sim t_d = 700 \text{ yr}$  (assuming a lobe size of 540 AU, see §4), and allowing as above for an increase in the mass by  $\sim 10$  due to opacity and missing flux corrections, we find an upper limit of  $\dot{M}_{out} \sim 2 \times 10^{-7} M_{\odot} \text{ yr}^{-1}$ . If instead  $t_{flow} \sim 10t_d$  with no correction applied to the mass estimate we obtain  $\dot{M}_{out} \sim 2 \times 10^{-9} M_{\odot} \text{ yr}^{-1}$ .

## 4.2. Discussion

The values calculated above show that the outflow is of low mass, and correspondingly weak in its momentum, energy, mechanical luminosity, and force, when compared to other outflows (Bontemps et al. 1996; Wu et al. 2004). In fact, L1014-IRS is the lowest luminosity source to date with a detectable bipolar molecular outflow, of 292 outflows with well determined bolometric luminosity  $L_{bol}$  (Wu et al. 2004). Our data suggests that L1014-IRS is not edge on, and so its  $L_{bol}$  estimate is reasonable. Even allowing for an upward revision of the outflow parameters due to

uncertainties in the CO opacity and missing flux, the outflow mass is at least an order of magnitude lower than any other outflow; the lowest previously reported has  $M \sim 10^{-3} M_{\odot}$  (B1-IRS; Wu et al. 2004). The derived values of  $L_{bol}$ ,  $M$ ,  $L_m$ , and  $F_{obs}$  are consistent with extrapolation of the relations among these quantities found for other outflows (e.g., Wu et al. 2004). L1014-IRS appears to be a weaker version of a typical outflow. The low values might suggest that the emission is in fact due to bound motions and not outflow emission, so using a size of 540 AU and velocity of  $3.6 \text{ km s}^{-1}$  we estimate an interior mass of  $\sim 4 M_{\odot}$  is required for bound motions, significantly larger than the core mass within the same radius ( $< 0.5 M_{\odot}$ ; Huard et al. 2005).

For comparison, the outflow from the low luminosity Class 0 protostar IRAM 04191+1522 ( $L \sim 0.15 L_{\odot}$  cf.  $0.09 L_{\odot}$  for L1014-IRS; Andre, Motte & Bacmann 1999) is large ( $> 14000 \text{ AU}$ ) with  $M \geq 0.03 M_{\odot}$  (Lee et al. 2002 from BIMA data) and  $F_{obs} \sim 2 \times 10^5 M_{\odot} \text{ km s}^{-1} \text{ yr}^{-1}$  (Andre et al. 1999). Unlike L1014-IRS, the CO outflow from IRAM 04191 is well detected with the IRAM 30-m over a larger velocity range, up to  $10 \text{ km s}^{-1}$  from the line center. The implied accretion rate, which follows directly from  $F_{obs}$ , is over two orders of magnitude greater for IRAM 04191. In addition, IRAM 04191 shows clear evidence for infall in mm transitions of CS and is bright and extended in mm molecular lines such as  $\text{N}_2\text{H}^+$  (Belloche et al. 2002; Crapsi et al. 2005). So although L1014-IRS and IRAM 04191 have similar low luminosities and are embedded in dense cores, the properties of their outflows and cores show significant differences, which may signify different pathways to formation, and different end results. Its outflow properties suggest that L1014-IRS has a low accretion rate for an embedded source, and we can speculate that it is either (i) close to finishing its main accretion phase, or (ii) its accretion rate is intrinsically low. Either scenario implies that L1014-IRS will remain a very low mass object, and it may be the first example of an embedded proto-brown dwarf. Further information, such as a near-infrared spectral classification, is needed to address its evolutionary state and future.

If L1014-IRS is indeed a proto-brown-dwarf, then our results suggest that BDs can form in a broadly similar manner to low mass stars (cf., the recent detection of outflowing gas from the young brown dwarf  $\rho \text{ Oph } 102$  by Whelan et al. (2005)), but that there might be significant differences in the details, by comparison with IRAM 04191. Alternatively the differences between L1014-IRS and IRAM 04191 might simply reflect differences in the mass and evolutionary state from one low-luminosity object to the next.

## 5. Summary

We have used the SMA to search for CO  $J = 2 \rightarrow 1$  outflow emission from L1014-IRS. The results are as follows:

1. A low velocity ( $< 4 \text{ km s}^{-1}$ ) compact bipolar CO outflow has been discovered centered on L1014-IRS, which directly associates L1014-IRS with the globule L1014 at  $\sim 200 \text{ pc}$  and confirms its low luminosity ( $\sim 0.09 L_{\odot}$ ).
2. L1014-IRS is the lowest luminosity and perhaps the lowest mass source known to be driving a bipolar molecular outflow.
3. The CO outflow is one of the smallest known in size ( $\sim 500 \text{ AU}$ ), mass ( $< 10^{-4} M_{\odot}$ ), and energetics (e.g.,  $F_{\text{obs}} < 10^{-7} M_{\odot} \text{ km s}^{-1} \text{ yr}^{-1}$ ). These values are consistent with the trends observed between them for large samples.

T. L. B. acknowledges support from the SMA Fellowship Program. The work of A. C. was supported by a Smithsonian Predoctoral Fellowship. P. C. M. acknowledges support from NASA Origins of Solar Systems Program Grant NAG 5-13050. We thank Mario Tafalla for obtaining the 30-m data. We extend special thanks to those of Hawai’ian ancestry on whose sacred mountain we are privileged to be guests.

## REFERENCES

- André, P., Motte, F., & Bacmann, A. 1999, *ApJ*, 513, L57
- Bally, J., & Lada, C. J. 1983, *ApJ*, 265, 824
- Belloche, A., André, P., Despois, D., & Blinder, S. 2002, *A&A*, 393, 927
- Bontemps, S., André, P., Terebey, S., & Cabrit, S. 1996, *A&A*, 311, 858
- Cabrit, S., & Bertout, C. 1990, *ApJ*, 348, 530
- Crapsi, A., et al. 2005, *A&A*, 439, 1023
- Ho, P. T. P., Moran, J. M., & Lo, K. Y. 2004, *ApJ*, 616, L1
- Huard, T.L., et al. submitted to *ApJ*
- Lee, C.-F., Mundy, L. G., Stone, J. M., & Ostriker, E. C. 2002, *ApJ*, 576, 294
- Leung, C. M., Kutner, M. L., & Mead, K. N. 1982, *ApJ*, 262, 583
- Levreault, R. M. 1988, *ApJS*, 67, 283
- Parker, N. D. 1988, *MNRAS*, 235, 139

- Parker, N. D., Padman, R., & Scott, P. F. 1991, MNRAS, 252, 442
- Visser, A. E., Richer, J. S., & Chandler, C. J. 2001, MNRAS, 323, 257
- Whelan, E. T., Ray, T. P., Bacciotti, F., Natta, A., Testi, L., & Randich, S. 2005, Nature, 435, 652
- Wu, Y., Wei, Y., Zhao, M., Shi, Y., Yu, W., Qin, S., & Huang, M. 2004, A&A, 426, 503
- Young, C. H., et al. 2004, ApJS, 154, 396



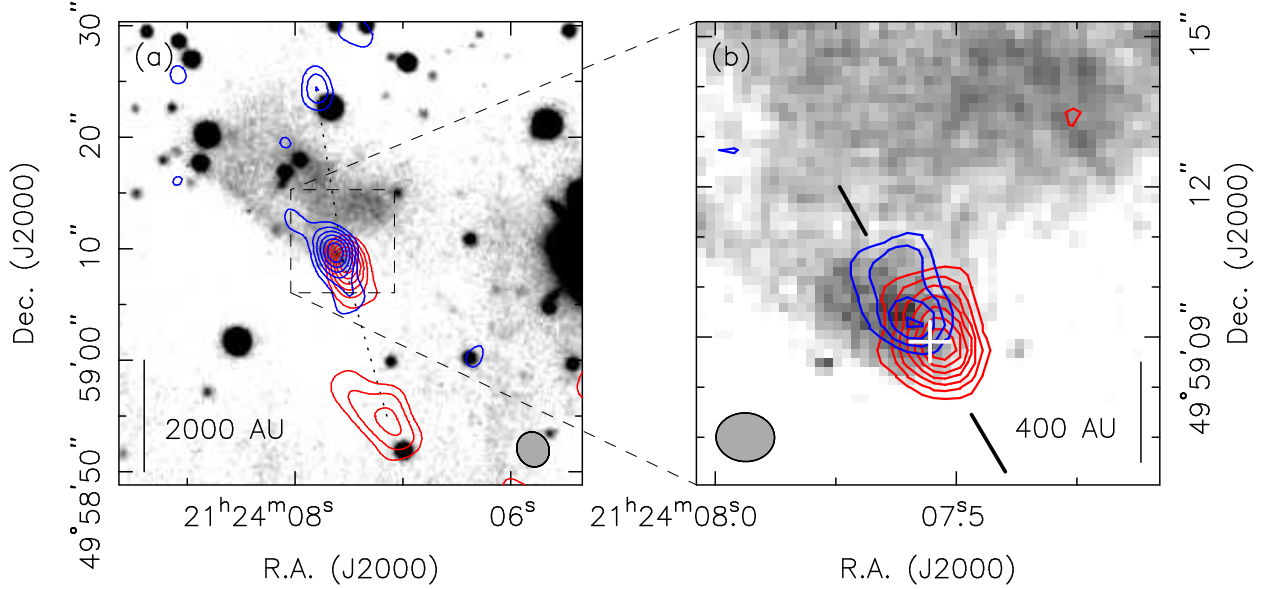


Fig. 1.— Integrated intensity maps of CO  $J = 2 \rightarrow 1$  emission toward L1014, overlaid on a H band image ( $1.6 \mu\text{m}$ ) from Huard et al. 2005. (a): Blue (red) contours represent blue (red) shifted emission between velocities (LSR) of  $2.0$  and  $3.8 \text{ km s}^{-1}$  ( $4.9$  and  $7.0 \text{ km s}^{-1}$ ). The images were made with natural weighting, and have been tapered with a  $3''$  Gaussian. The contours are  $2, 3, 4, \dots \times$  the rms of  $0.16 \text{ Jy/beam}$  ( $0.25 \text{ Jy/beam}$ ) for the blue (red) shifted emission. The dotted lines are drawn from L1014-IRS to the peaks of the blue and red shifted emission that are spatially offset from L1014-IRS. The beam of  $3''.19 \times 2''.84$ , P.A.  $24.7^\circ$  is shown at lower right. (b): As for (a), but with integration over  $2.2$  and  $3.4 \text{ km s}^{-1}$  (blue) and  $5.2$  and  $7.5 \text{ km s}^{-1}$  (red). The images were made with Briggs' robust parameter of  $0$ . The contours are  $2, 3, 4, \dots \times$  the rms of  $0.08 \text{ Jy/beam}$  ( $0.12 \text{ Jy/beam}$ ) for the blue (red) shifted emission. The position and uncertainty of L1014-IRS is indicated with the white cross, and the beam of  $1''.17 \times 0''.97$ , P.A.  $88.1^\circ$  is shown at lower left. The position-velocity cut shown in Fig. 2 which passes through L1014-IRS is indicated by the two short black lines either side of the outflow with P.A.  $\sim 30^\circ$ .

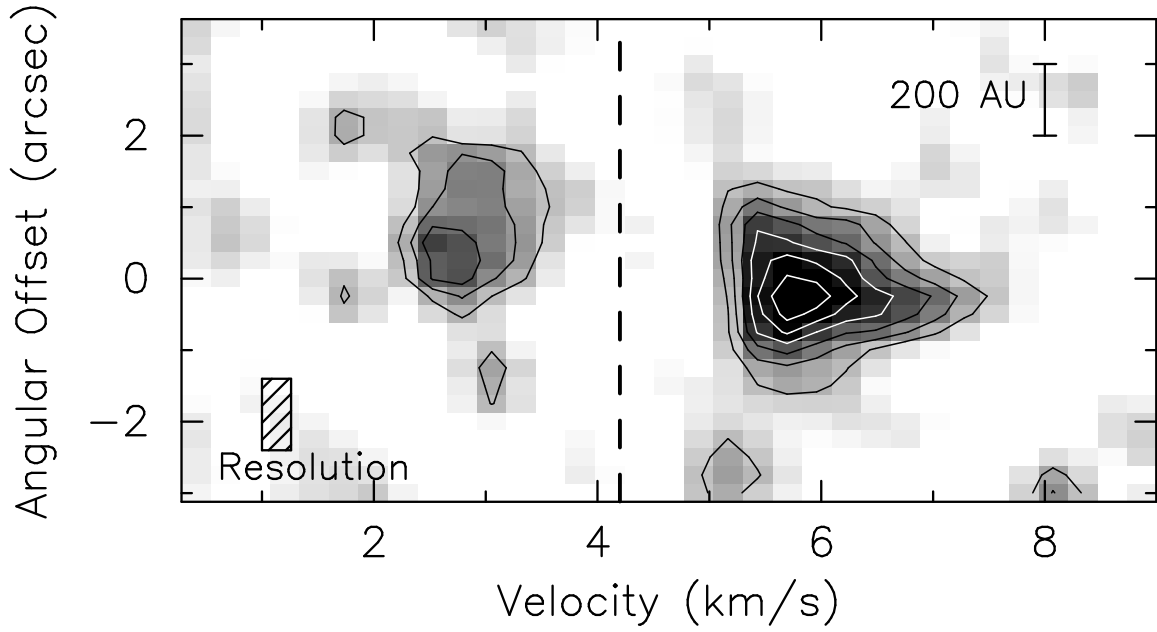


Fig. 2.— Position-Velocity (P-V) diagram for CO  $J = 2 \rightarrow 1$  emission. The direction of the cut is indicated on Fig. 1(b), and offsets are relative to L1014-IRS. The cloud systemic velocity marked by the thick dashed line. The contours are 2, 3, 4, ...  $\times$  the rms of 0.08 Jy/beam.

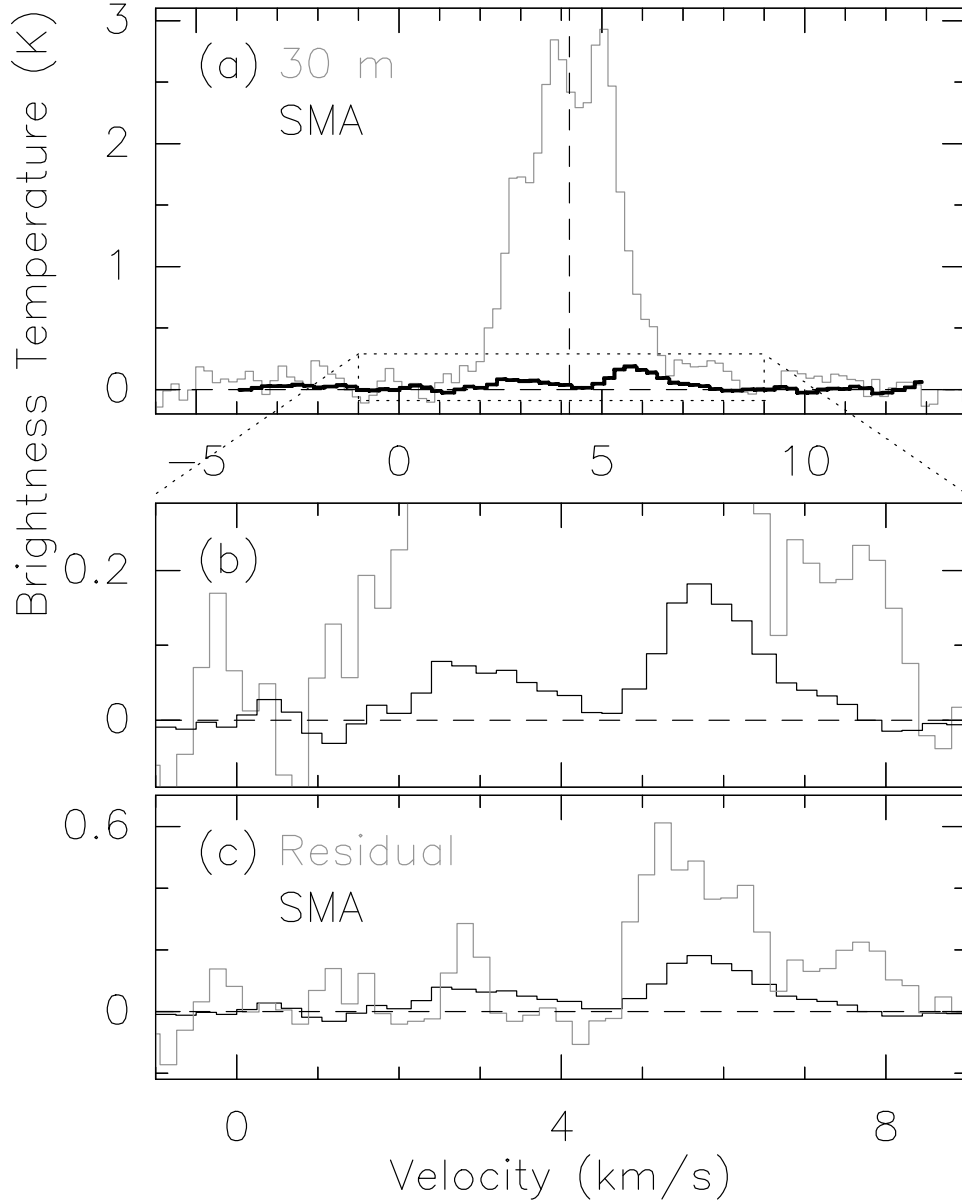


Fig. 3.— Comparison of the IRAM 30-m and SMA CO  $J = 2 \rightarrow 1$  observations of L1014. Panel (a) shows the 30-m (11'' beam) and SMA spectra (convolved with a 4'' beam and scaled by the ratio of the 30-m and SMA beam areas) at the position of L1014-IRS. Panel (b) shows an enlarged version of a portion of panel (a) for clarity. Panel (c) shows again the SMA spectrum, and the difference (“Residual”) between the 30-m center spectrum and a mean spectrum made by combining spectra at 11'' offset positions in a ring around the center.